CHAPTER 134

SEA BED STABILITY ON A LONG STRAIGHT COAST

E. Damgaard Christensen[1], R. Deigaard[2], J. Fredsøe[3]

Abstract

A stability analysis is used to investigate the development of large-scale periodic bottom topographies on a straight uniform coast. The work is an extension of the work by Hino (1974) and (1976), and special attention is paid to improve and refine the description of the sediment transport. The effect of the bed slope on the bed load sediment transport turns out to be very important. Further, the behaviour of suspended sediment is described by introducing lag effects that modify the predictions of the wave length considerably.

1 INTRODUCTION

A coast is often irregular. Even a long straight coast can be very non-uniform in the longshore direction. A longshore bar can be crossed by more or less regularly spaced rip channels or it may be sinuous. Lippmann and Holman (1990) have shown several examples of different configurations of a coast that on a large scale is almost straight.

Here the formation of large-scale periodic bottom topographies is investigated by applying a linear stability analysis. The basic idea is to give a uniform bed a small perturbation. This perturbation affects the hydrodynamics and the sediment transport which again influences the bed form. It is then investigated whether the perturbation will grow in time or die out. For several different perturbations the one with the fastest growth is the one that would be expected to be dominant if the coast was given a random perturbation.

The linear stability analysis is only valid for an infinitisemal small bed perturbations, but it is expected that some of the main features of the fastest growing perturbation would also be found in the coastal forms that actually emerge.

[1]Ph.D-student, [2]Associated Professor, [3]Professor: ISVA, Danish Technical University, DK-2800 Lyngby, Denmark

An investigation of this kind was carried out by Hino (1974) and (1976). Hino used a very simple model for the sediment transport, and the present work is an extension of that analysis, investigating the effect of more sophisticated sediment transport descriptions, including the effect of the bed slope, and the gradual adaption of the suspended load transport due to changing hydrodynamic conditios.

2 DESCRIPTION OF WAVES, CURRENTS AND SEDIMENT TRANSPORT

The analysis considers a uniform, plane (constant slope) coastal profile with a small perturbation. The geometry and coordinate system are shown in figure 1. The "breaker line" is here defined as the line where regular waves with a deep water wave height equal to the root-mean-square wave height for irregular waves at deep water would start to break.

The chosen models for waves, currents, and sediment transport are as simple as possible, yet still represent the relevant physical processes.

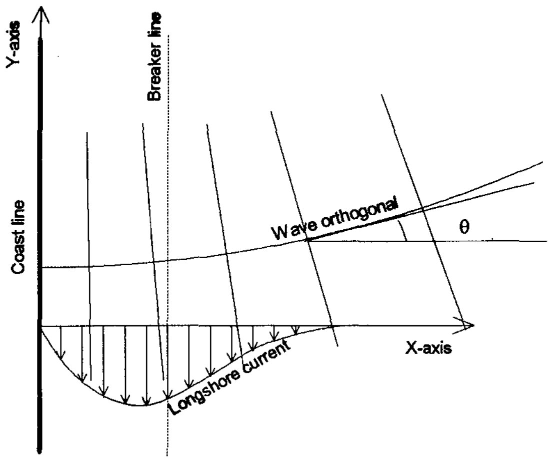

Figure 1 *The figure shows the definition of the x and y-directions*

2.1 Wave description

The waves are assumed to be irregular with Rayleigh-distributed wave heights. The breaking process is described by the theory of Battjes (1972), where the local wave height distribution is taken as the Rayleigh distribution where the wave heights are limited by the water depth: $H_b = 0.8\ h$. This model is expected to give satisfactory results on a gently sloping, monotone beach profile. The assumption of irregular waves gives a smooth distribution of the driving forces and the longshore current distribution.

The waves are described by linear shallow water theory, which is expected to give a reasonable representation of the depth refraction and radiation stress variation in the surf zone. The wave conditions are specified at the breaker line x_b where uniform waves would start to break.

2.2 The current description

The current is described by the depth-integrated equations for conservation of mass and momentum:

Momentum in the x-direction:

$$\rho\frac{\partial u(h+\eta)}{\partial t} + \rho\frac{\partial (h+\eta)u^2}{\partial x} + \rho\frac{\partial (h+\eta)vu}{\partial y} + \frac{\partial s_{xx}}{\partial x} + \frac{\partial s_{xy}}{\partial y} = -\rho g(h+\eta)\frac{\partial \eta}{\partial x} - \tau_{bx} \tag{1}$$

Momentum in the y-direction:

$$\rho\frac{\partial v(h+\eta)}{\partial t} + \rho\frac{\partial (h+\eta)uv}{\partial x} + \rho\frac{\partial (h+\eta)v^2}{\partial y} + \frac{\partial s_{xy}}{\partial x} + \frac{\partial s_{yy}}{\partial y} = -\rho g(h+\eta)\frac{\partial \eta}{\partial y} - \tau_{by} \tag{2}$$

Mass conservation:

$$\frac{\partial (h+\eta)}{\partial t} + \frac{\partial u(h+\eta)}{\partial x} + \frac{\partial v(h+\eta)}{\partial y} = 0 \tag{3}$$

u and v are the depth-averaged velocities, η is the mean surface elevation, h is the still water depth, s_{xx}, s_{xy} and s_{yy} are the radiation stresses, and τ_{bx} and τ_{by} are the components of the bed shear stress.

The flow resistance is described by a simple model for the turbulent interaction between the current and the oscillatory wave boundary layer, Fredsøe (1981), see also Fredsøe and Deigaard (1992), pp 56-62. This gives a flow resistance represented by a logarithmic velocity profile, but with an increased bed roughness due to the wave boundary layer.

2.3 Sediment transport

The morphological development is described by the conservation equation for sediment:

$$(1-n)\frac{\partial h}{\partial t} = \frac{\partial q_{totx}}{\partial x} + \frac{\partial q_{toty}}{\partial y} \tag{4}$$

where q_{totx} and q_{toty} is the total sediment transport in x and y-directions and n the porosity.

One of the main purposes of this study has been to consider the influence of the sediment transport model on the morphological stability. Three approaches have been investigated.

<u>The simple approach</u>

As a first approach the sediment transport rate is taken to be proportional to the local current velocity. This is the model used by by Hino (1974).

$$\boldsymbol{q_t} = C_s \boldsymbol{V} \tag{5}$$

where $\mathbf{q}_t$ is the sediment transport vector and $\mathbf{V}$ is the depth-averaged velocity. The coefficient C_s is taken to be constant.

<u>The bed load transport model</u>

The transport of sand is composed of bed load transport and suspended load transport, where the bed load transport q_b is determined by the local instantaneous bed shear stress, from the combination of waves and current.

The dimensionless bed load transport Φ_b can be expressed as a function of the dimensionless bed shear stress, the Shields parameter θ. The formula of Meyer-Peter and Müller (1948) has been applied:

$$\Phi_b = 8(\theta' - \theta_c)^{\frac{3}{2}}$$

$$where \quad \Phi_b = \frac{q_b}{\sqrt{(s-1)gd^3}} \quad and \quad \theta = \frac{\tau_b}{(s-1)gd} \tag{6}$$

θ_c is the critical Shields parameter, $\theta_c = 0.05$, d is the grain diameter, and s is the relative density of the sediment.

If the bed is sloping, there is an additional down slope component of the sediment transport. When the transport is directed up (or down) the slope, gravity gives a down slope force component that has to be added to the force from the shear stress, giving a correction to the critical Shield's parameter:

$$\theta = \theta_c - \alpha \frac{\partial h}{\partial x} \tag{7}$$

where α is from 0.05 to 0.1 cf Fredsøe and Deigaard (1992).

When the transport is along the slope, the down slope component of the gravity deflects the direction of the transport by the angle ψ, which can be found as: (Engelund and Fredsøe 1982)

$$\tan\psi = \frac{1}{1.6\sqrt{\theta}} \frac{\partial h}{\partial y} \tag{8}$$

For an arbitrary angle between the bed shear stress vector and the strike of the slope the effect of a longitudinal and transverse slope is combined.

The bed load transport is determined by the instantaneous bed shear stress, and is then averaged over the wave period. The instantaneous bed shear stress is determined from the flow resistance model, using the wave friction factor f_w on the combination of the near-bed wave-orbital velocity and the mean flow velocity at the top of the wave boundary layer.

The suspended load transport

The suspended sediment moves away from the bed in the water column. When the hydrodynamic conditions change, it takes some time for the grains to be entrained in the water column or be deposited. Therefore, it takes some time/length for the suspended load transport to be adjusted to a variation in the hydrodynamic conditions.

The transport of the suspended sediment is calculated by the models of Fredsøe et al (1985) and Deigaard et al. (1986) which includes the turbulent interaction between the wave boundary layer and the current and takes the turbulence generated by wave breaking into account. For the suspended sediment transport calculations the modelling system Litpack of the Danish Hydraulic Institute has been applied.

The gradual adaptation of the transport to a gradient in the hydrodynamic conditions is represented by an adaptation length L_s, by which the transport lags behind the development in the forcing terms. L_s is estimated by the time it takes for a grain to settle from the concentration profile of suspended sediment:

$$L_s = \alpha \frac{z_c}{\omega_s} V_0 \tag{9}$$

where z_c is the height from the bed of the centroid of the sediment concentration profile, w_s is the settling velocity of the sediment and V_0 is the mean flow velocity and α is a coefficient, which is expected to be of the order 1.

3 ZERO ORDER SOLUTION AND FIRST ORDER EQUATIONS

The stability analysis is performed by using a perturbation method. First the equilibrium conditions for the longshore current and the set up are calculated. The equilibrium is perturbated, and the perturbated equations are found. Here the difference between the steady solution and the solution with a small perturbation is called the perturbated solution or the first order solution and the steady solution is called the zero order solution. If all types of perturbations of the bottom will die out in time, the equilibrium is stable. If the perturbation grows, the bed is unstable.

To calculate the zero order solution - the profile without any bed undulations - is actually a project by itself. It usually requires a detailed on offshore description including undertow etc. This cross shore sediment transport is considered to be unimportant for the further development of sand bed undulations, and for reasons of simplicity it has been assumed that a coast with a constant slope is an equilibrium profile for the bottom.

3.1 The steady solution

The equations in section 2.1 are solved in the steady state. This means that U, V, η, h only depends on x, because the initial conditions are described by parallel bottom contours and a constant slope of the bottom. By this U and all the derivatives with respect to y is equal to zero.

When the description of the waves given by Battjes (1972) is used, a smooth set up is found from equation (1). The set up is a function of the angle of the incoming waves, the percentage Q_b of the waves that break or have broken and the root-mean-square H_{rms} of the remaining waves.

The flow resistance is described by the simple model for turbulent interaction between the wave and current boundary layer, which gives an increased flow resistance for the flow expressed as an increase in the bed roughness. The flow resistance for the current is almost quadratic.

3.2 First order equations

When the steady solution is found, the bed is given a little perturbation. This perturbation affects the hydrodynamics. The response time concept is applied. The idea behind the response time concept is that the bottom perturbation will cause immediate changes of the velocities in the x- and y-directions, but quick changes in the flow motion will not result in a response from the bottom. Thus the hydrodynamics are considered to be quasi-steady, and it is only the time variation of the bed level that is included in the description.

The total velocity field, water elevation, and water depth can be expressed by:

$$\left.\begin{aligned} U &= u'(x,y) \\ V &= V_0(x) + v'(x,y) \\ \eta &= \eta_0(x) + \eta'(x,y) \\ h &= h_0(x) + h'(x,y,t) \end{aligned}\right\} \qquad (10)$$

The first order perturbated equations can be found by substituting (10) into (1)-(4). All terms of higher order than one will then be omitted. The zero order terms will automatically fulfill these equations and can be cancelled out. With this we obtain equations that only contain first order terms.

The gravitational acceleration g and the distance from the shore to the breaker line L_B are used to make the equations non-dimensional. The dimensionless variables are written,

$$x \rightarrow \frac{x}{L_B}, \quad k \rightarrow k \cdot L_B, \quad c \rightarrow \frac{c}{\sqrt{gL_B}}, \quad q \rightarrow \frac{q}{\sqrt{gL_B}L_B} \qquad (11)$$

Each of the four differential equations can be put on a form as:

$$\begin{aligned} &\frac{\partial w_i}{\partial t} + A_{i1}\frac{\partial u}{\partial x} + A_{i2}\frac{\partial u}{\partial y} + a_i u + B_{i1}\frac{\partial v}{\partial x} + B_{i2}\frac{\partial v}{\partial y} + b_i v \\ &+ C_{i1}\frac{\partial \eta}{\partial x} + C_{i2}\frac{\partial \eta}{\partial y} + c_i\eta + D_{i1}\frac{\partial h}{\partial x} + D_{i2}\frac{\partial h}{\partial y} + d_i h + D^*_{i1}\frac{\partial^2 h}{\partial x^2} + D^*_{i2}\frac{\partial^2 h}{\partial y^2} + D^*_{i12}\frac{\partial^2 h}{\partial x \partial y} = 0 \end{aligned} \qquad (12)$$

where i is the number of equation. w_i is the variable that is derived with time in the equation, $w_4 = h$, for the other variables this term is cancelled out due to the response time concept. The coefficients in (12) depends on the zero order solution and the description of the sediment transport.

4 SOLVING THE EQ. BY FINITE DIFFERENCES

The equations are solved numerically by finite differences. When the assumption of periodic conditions in the y-directions is applied, the dependent variables can then be written as:

$u = U(x)\exp(iky)$ **(13)**

$v = V(x)\exp(iky)$ **(14)**

$\eta = Z(x)\exp(iky)$ **(15)**

$h = H(x)\exp(pt + iky)$ **(16)**

Figure 2 shows a sketch of how the finite difference scheme is applied. The node points are distributed over three times the width of the breaking zone. The start of the breaking zone is defined as the line where regular waves with a wave height equal to H_0 would start to break.

In figure 2 x_b is the distance from the coast line at still water level to the start of the "breaking line". x_i is the distance between the still water line and the actual water line. The total width of the breaking zone L_b is thus the sum of x_i and x_b.

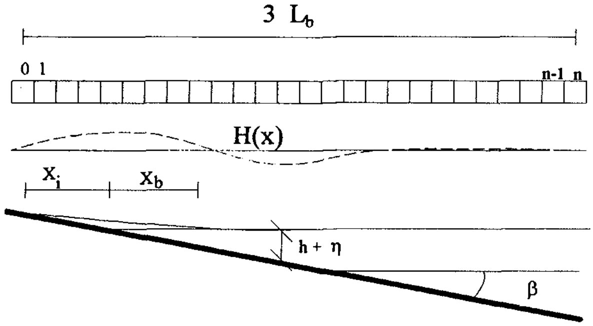

Figure 2 Sketch of the finite difference approximation. The points are distributed over three times the width of the "breaking zone" L_b

Solution method

The expressions in (13) to (16) are substituted into (12) by which four ordinary differential equations for U, V, Z and H are obtained. These are solved by introducing second or fourth order finite difference approximations for the derivatives of U, V, Z and H. For node points at the boundaries forward/backward finite differences are used, and for the node points at 2 and n-2 second order finite differences are used for terms that are not given on the boundary. As boundary conditions U, V, Z and H are set equal to 0 at the right boundary (deep water), and U is set equal 0 at the coast line, $x = -x_i$, see figure 2.

With this, a matrix-equation is found:

$$\underline{A}\mathbf{x} = \mathbf{px} \tag{17}$$

The vector **x** has the dimension 4(n-1) and it has the form:

$$\mathbf{x} = (U_1, U_2, .. ,U_{n-2}, U_{n-1}, V_1, V_2, .. ,V_{n-2}, V_{n-1}, Z_1, Z_2, .. , Z_{n-2}, Z_{n-1}, H_1, H_2, .. H_{n-2}, H_{n-1})$$

px is a vector that originates from the terms derived with respect to time in (12).

$$\mathbf{px} = (0, 0, .. ,0, 0, 0, 0, .. ,0, 0, 0, 0, .. , 0, 0, pH_1, pH_2, .. pH_{n-2}, pH_{n-1})$$

By use of gauss-elimination equation (17) is transformed to an eigenvalue problem for **H** .

Matrix $\underline{\mathbf{A}}$ contains of 16 sub-matrices. These are named $\mathbf{A}_i$, $\mathbf{B}_i$, $\mathbf{C}_i$, $\mathbf{D}_i$:

$$\underline{A} = \begin{pmatrix} A_1 & B_1 & C_1 & D_1 \\ A_2 & B_2 & C_2 & D_2 \\ A_3 & B_3 & C_3 & D_3 \\ A_4 & B_4 & C_4 & D_4 \end{pmatrix} \tag{18}$$

The matrices **A**, **B**, **C** and **D** contains elements, respectively, for **U**, **V**, **Z** and **H**. The index refers to the equations. 1 for the x-momentum, 2 for y-momentum, 3 for conservation of mass and 4 for conservation of sediment. When the matrix $\underline{\mathbf{A}}$ has been calculated, it is reduced to a triangular matrix except the last submatrix $\mathbf{D}_4$. The form of the matrix-equation is now:

$$\begin{pmatrix} A_1* & B_1* & C_1* & D_1* \\ 0 & B_2* & C_2* & D_2* \\ 0 & 0 & C_3* & D_3* \\ 0 & 0 & 0 & D_4* \end{pmatrix} \begin{pmatrix} U \\ V \\ Z \\ H \end{pmatrix} = -p \begin{pmatrix} 0 \\ 0 \\ 0 \\ H \end{pmatrix} \tag{19}$$

The matrices' $\mathbf{A}_1*$, $\mathbf{B}_2*$ and $\mathbf{C}_3*$ are all upper triangular matrices. It is only possible to obtain a solution to equation (19) when **H** is a solution to the eigenvalue problem defined by following equation:

$$\mathbf{D}_4*\cdot\mathbf{H} = -\,\mathbf{p}\mathbf{H} \tag{20}$$

(20) is complex in both matrix, vector, and eigenvalue. It is solved by use of standard procedures for complex eigenvalue problems. The solution to the eigenvalue problem gives n-1 eigenvalues $\lambda_1, \ldots, \lambda_{n-1}$. Each of the eigenvalues defines a solution to the eigenvalue problem, which also give n-1 eigenvectors $\mathbf{H}_1$ .. $\mathbf{H}_{n-1}$.

It is now possible to find the solution that gives the fastest growth rate of the bed perturbation that is determined by the largest real part of $p_i = -\lambda_i$, cf. eq. (16). When the eigenvector $\mathbf{H}_i$ for the fastest growing mode has been found, the solution for U, V and Z are found by using back substitution.

The calculations are made for several different values of k in order to determine the wave number k that gives the largest real part of p and thus the fastest growing perturbation. This bar pattern is expected largely to be the bed form that actually emerges.

Another result that comes from the eigenvalue problem is the migration velocity, which is:

$$c_h = \frac{-Im(p)}{k} \tag{21}$$

5 RESULTS

As can be seen in fig. 3 the simple sediment transport model does not give a maximum for the growth factor Re(p). Fig. 4 shows the most unstable bed configuration for different values of k. It can be seen that as k increases the bars are situated closer to the coastline.

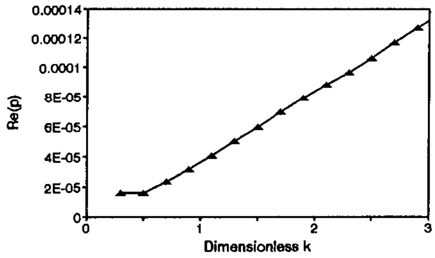

Figure 3 The real part of the growth factor p as a function of the wave number k. The simple sediment transport model was used. H_b*=3 m, T=10 s,* $\beta = 2.5°$ *and* $\theta_b = 10.0°$.

For large longshore wave numbers the bed forms are thus embedded in the nearshore region where the longshore current is growing linearly with the distance from the shoreline, see figure 4. Under these conditions there is no lower limit for the wave length of the most unstable perturbation and the stability analysis cannot predict the emerging of a bed topography.

An explanation for this behaviour is as follows. When the bars are situated closer to the coast line, the area of a bar is decreased as k^{-2}, whereby the amount of sediment needed for the instability mechanism is reduced with k^{-2}. Close to the coast line the zero order velocity profile is almost linear and the sediment transport is proportional to the zero order velocity. The sediment transport hereby reduces by ~ k^{-1} as the bars are situated closer to the coast line. This gives:

$$Re(p) \propto k^{-1}/k^{-2} = k$$

This agrees with the result shown in figure 3.

When the bed load transport model is used a maximum for Re(p) is found, see figure 5. The dimensionless wave number k is found to be around 1.0 to 1.2 for waves for an incoming angle at the breakerline between 8° and 12°. For lower angles the wave number k becomes very small for the maximum of Re(p). For $\theta_b = 0°$ it is impossible to get any results due to the use of a quadratic resistance law which also has influence on the results for small angles of θ_b.

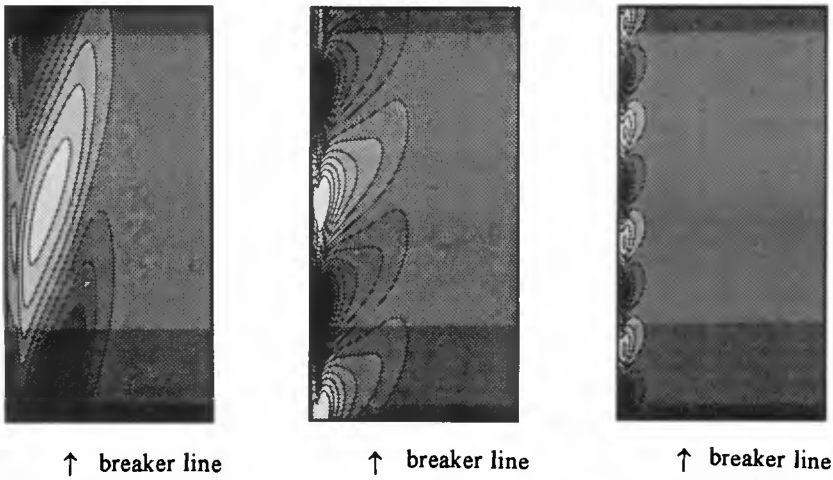

k = 1 *k = 2* *k = 4*

Figure 4 An example of the perturbation h, for three different wave numbers k, H_b =3 m, T=10 m, $\beta = 2.5°$ and $\theta_b = 10.0°$.

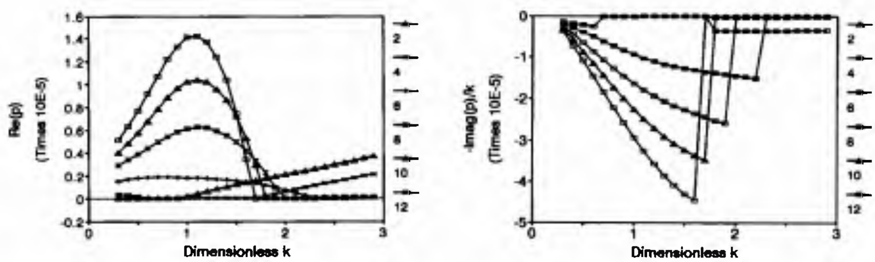

Figure 5 The real part of the growth factor p and the translation celerity as a function of the wave number k for six different angles. The bed load model was used. H_b=3 m, T=10 s, $\beta = 2.5°$

Illustrations of the 1. order bed topography, 1. order velocity field and the "total" meandering current are shown in figure 6. The orientations of the bars disagree with the one seen on the photo in figure 7. On the photo the bars propagate from the coastline obliquely in the same direction as the current, the opposite is the case in the stability analysis. In another case, illustrated by a photo of Short (1994), the orientation of the bed forms agree with the present stability analysis. Johnson et al. (1994)

modelled the current and mophological changes around an offshore breakwater for obliquely incoming waves. At the downstream side of the breakwater some bars developed that had the same orientation as those in the present study. It has not been possible to find a final explanation for the determination of the orientation.

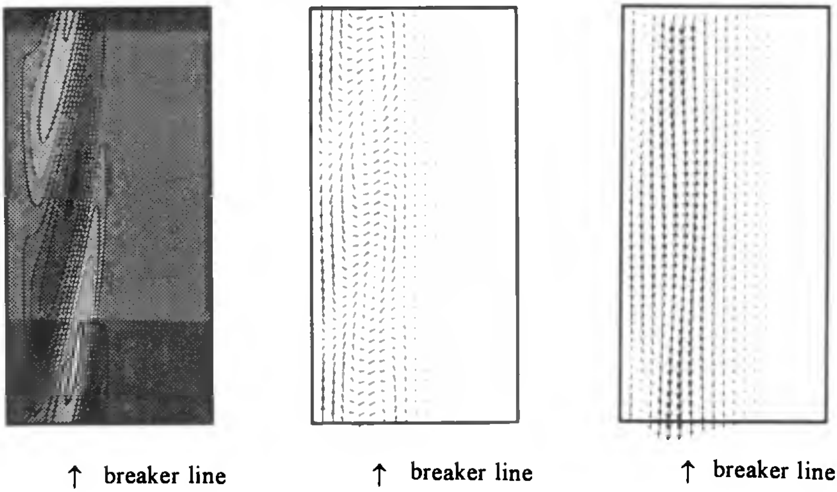

Figure 6 An example of the perturbation h, the 1. order current and the "total" (0. and 1. order) meandering current. $\theta_b = 8.0°$, $k = 1.2$, $H_b = 3$ *m,* $T=10$ *m and* $\beta = 2.5°$. *For the meandering current the maximum of h was set to 2 m. The scoured area is shown by the light colour*

Figure 7 A photo of large periodic bottom topographies at the island Sylt, Wadden Sea Denmark/Germany, H. Dette (1994).

Figure 8a shows the dependence on the grain size. When the grain size increases the maximum of Re(p) decreases and the wave length of the most unstable perturbation increases.

The perturbation of the bed modifies the wave field. This influences on the radiation stresses and hereby on the hydrodynamics and the sediment transport. A comparison between the effects coming from the bed slope, the modification of the wave field due to the perturbation and the current is shown in figure 8b. When the modification of the wave field due to the perturbation is excluded the lowest curve is obtained where the maximum is situated at the same wave number k as for the full bed load model. When the effect of the bed slope and the effect of the modified wave field are excluded, the maximum for Re(p) is situated at a larger wave number k. Here a maximum is obtained in contrast to the simple model. This shows that a more refined model for the sediment transport gives a maximum even if the bed slope is not taken into account.

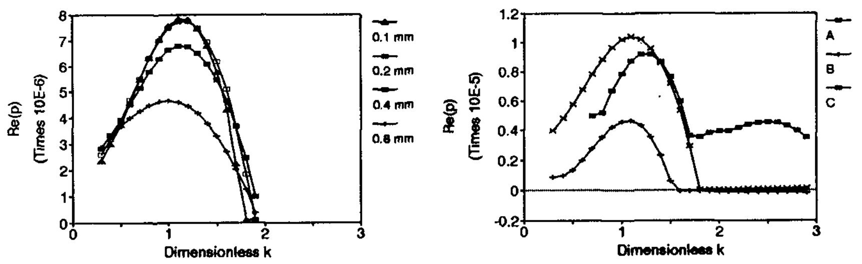

8a *8b*

Figure 8 The figure shows the dependency of the grain size - 8a -, and the stability curve when the slope and/or the modification of the wave field are excluded - 8b. A : no slope and no modification of the wave field, B: no modification of the wave field, C: the full bed load model

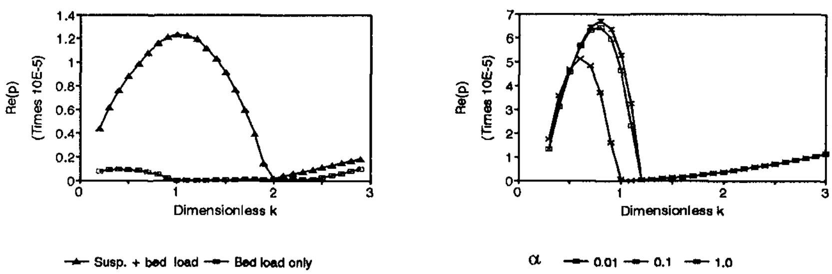

Figure 9 Here the suspended load is included, the figure on the left hand side is found for $\theta_b = 5.0°$ and for the figure at the right hand side $\theta_b = 10°$. $H_b = 3\ m$, $T = 10\ m$ and $\beta = 2.5°$.

Figure 9 shows the results when the suspended load is incorporated. For θ_b = 5.0° the maximum for Re(k) moves to a bigger dimensionless k, while we get the opposite result for θ_b = 10°. When the suspended load becomes dominant, it moves the maximum of Re(p) to a lower dimensionless k, and the growth rate increases.

For θ_b = 10° the effect of a phase lag is shown too. This has a stabilizing effect on the growth rate especially with big wave numbers.

6 CONCLUSIONS

A linear stability analysis has been used to investigate the formation of large scale periodic bottom topographies. In the analysis the effects from the slope due to the perturbation of the bed are incorporated.

When a simple sediment transport formulation is used, taking the sediment transport to be proportional to the velocity, a maximum on the stability curve is not found, and the instability of the bed forms increases with the alongshore wave number.

The bed slope affects what kind of topography that will emerge and gives a spacing between the rips of about six times the width of the breaking zone. By including the suspended load this distance decreases for small angles of the incoming waves and increases for large angles. The phase lag in the suspended load gives a smaller growth rate and a longer length of the bar.

The modification of the wave field, due to the perturbation, increases the growth rate and gives a smaller bar length.

The stabilizing effects are the slope of the bed, large grain size and phase lag in the suspended load transport. The destabilizing effects are the longshore current, and the modification of the wave field due to the perturbation of the bed. Refraction and diffraction have not been investigated. These mechanisms could have an effect on the stability of the bars.

The resulting topography has been compared to field investigations and shows that the orientation of the bars sometimes but not always is the same as in this stability analysis.

ACKNOWLEDGEMENT

This work was founded jointly by the Danish Technical Research Council under the programme "Marin Teknik" and by the Commission of the European Communities, Directorate General for Science, Research and Development under MAST contract no. MAS2-CT92-0024 under the programme CSTAB.

REFERENCES

Deigaard R., Fredsøe J., and Brøker Hedegaard I. (1986):"Suspended sediment in the surf zone" Journal of Waterway, Port, Coastal and Ocean Engineering, ASCE, Vol. 112, No. 1, pp 115 - 128

Dette H. Private communications, (1994)

Engelund F. and Fredsøe J. (1982):"Hydraulic theory for alluvial rivers",Advances in Hydroscience, Vol 13 pp 183-215

Fredsøe J., Andersen O. H. and S. Silberg (1985):"Distribution of suspended sediment in large waves", J. of Waterway, Port, Coastal and Ocean Engineering Vol. 111, No 6,pp 1041-1059

Fredsøe J. and R. Deigaard (1992):"Mechanics of Sediment Transport in Coastal Regions", World Scientific, Singapore, 369 pages

Hino M. (1974):"Theory of formation of rip-current and cuspidal coast", Proc. 14th Int. Conf. on Coastal Eng., Copenhagen, Vol 1, page 901-919

Hino M. (1976):"Rip-current and coastal topography", Proc. 15th Int. Conf. on Coastal Eng., Honolulu, Vol 1, pp 1326-1341

Johnson H. K., Brøker I and Zysermann J. A. (1994):"Identification of relevant processes in coastal morphological modelling", 24th Int. Conf. on Coastal Eng., Kobe , Japan, Book of Abstracts, pp 448-449

Lippmann T. C. and Holman R. A. (1990): "The spatial and temporal variability of sand bar morphology", J. of Geophysical Research Vol. 95, No C7,pp 11575-11590, july 15

Meyer-Peter, E and Müller, R. (1948): "Formulas for bed-load transport ", Rep. 2nd Meet. Int. Assoc. Hydraul. Struct. Res., Stockholm 1948, pp 39-64

Short, Andrew D. (1994): Coastal Photograph, Jour. of Coastal Research, Vol 10 nr. 1, page 250